Turkish Journal of Electrical Engineering & Computer Sciences

http://journals.tubitak.gov.tr/elektrik/

Research Article

Turk J Elec Eng & Comp Sci
(2019) 27: 1922 – 1937

doi:10.3906/elk-1805-75

Fast nonsingular terminal decoupled sliding-mode control utilizing time-varying sliding surfaces

Ferhun YORGANCIOĞLU[1,*], **Soydan REDIF**[2]

[1]Department of Software Engineering, Faculty of Engineering, European University of Lefke, Lefke, Northern Cyprus
[2]Department of Electrical and Electronics Engineering, Faculty of Engineering, European University of Lefke, Lefke, Northern Cyprus

Received: 12.05.2018 • **Accepted/Published Online:** 22.01.2019 • **Final Version:** 15.05.2019

Abstract: In this paper, a fast form of nonsingular, terminal, decoupled, sliding-mode control, which utilizes time-varying sliding surfaces, is proposed for a class of fourth-order, single-input, multioutput, nonlinear systems. The novel control law features a fast term, in the manner of fast terminal sliding-mode control, which markedly improves the finite-time sliding-mode convergence speed near zero. Numerical simulation results, which are illustrated with a cart-pole inverted pendulum system and a ball-beam system, demonstrate that the proposed control law achieves, in general, favorable transient response and lower steady-state errors compared to state-of-the-art decoupled terminal sliding-mode control methods.

Key words: Sliding-mode control, terminal sliding mode, fast nonsingular terminal sliding mode, decoupled control, time-varying sliding surfaces, fourth-order systems

1. Introduction

Much attention has been devoted to the development of control methods for nonlinear systems, such as mechanical systems [1–4], robot manipulators [5, 6], aerospace systems [7], and power systems [8–10]. A significant portion of the literature has focused on the sliding-mode control (SMC) method due to its many advantages, including strong robustness, high control accuracy, computational simplicity, and ease of implementation [11, 12]. SMC is a type of variable-structure control method that uses a decision rule, more commonly known as a sliding surface (or switching manifold), and a discontinuous feedback control law with differing control structures [11]. The sliding surface dictates the particular type of continuous function that should be used for the current state-space location. The two main modes of operation constituting the SMC process are reaching mode and sliding mode. In the former, the system state is attracted and driven toward the sliding surface; then, in the latter, the state is constrained to traverse the surface towards the origin, which it reaches asymptotically using linear surfaces [11]. The sliding surface is chosen so as to minimize tracking errors and guarantee stability [13].

Generally, traditional SMC methods use linear sliding surfaces, the convergence time of which is infinite. Commonly known as terminal SMC (TSMC) [14, 15], an established approach for overcoming this problem has been to use a fractional-exponent term in the sliding-surface function. This gives finite-time convergence of the system states [16]. However, conventional TSMC controllers suffer from two potential problems: first, a negative (fractional) power in the nonlinear term results in an unbounded control magnitude as the state approaches

*Correspondence: fyorgancioglu@eul.edu.tr

equilibrium, namely the singularity problem [17, 18], and second, good convergence behavior cannot be assured when the system trajectory is at increased distances from the origin [19].

In [19], the authors proposed fast TSMC (FTSMC), which is based on the usage of an additional linear term in the sliding-surface function. This approach guarantees fast convergence but does not tackle the singularity problem [6]. Recent research has focused more on developing FTSMC while solving the singularity problem [1, 2, 5–7, 9, 10, 20].

Time-varying sliding surfaces (TVSSs) have been used to shorten the duration of the reaching mode [21–24], where SMC sliding surfaces are shifted and/or rotated. For example, the authors of [23] reformulate the sliding-surface slope in terms of fuzzy rules, called fuzzy SMC (FSMC). Also, FSMC-based methods have been introduced that minimize the set of required fuzzy rules with the aim of improving computational efficiency and reducing complexity, e.g., [24]. There, a simple but powerful FSMC method is proposed, which uses linear functions, which are derived from a one-dimensional (1-D) fuzzy rule base, to determine the slope of time-varying, sliding surfaces.

Applied to systems with coupling between two or more subsystems, or to higher-order systems, it would not be possible to achieve the same levels of performance using the aforementioned methods. For example, in a cart-pole system, there is coupling between the cart position and pole angular position, for which a centralized controller would be complex and may not produce acceptable performance. A popular approach to solving this problem is to decouple the system into second-order subsystems using a two-level decoupling strategy [25], called decoupled SMC (DSMC). By using two sliding surfaces—one per subsystem—these methods produce more effective and simpler controllers [26–28]. One of the subsystems is chosen as the primary system, for which the controller is designed using state information about the other (secondary) subsystem. Selection of the primary subsystem is problem dependent; e.g., in our cart-pole example, the pole is chosen as the primary subsystem since maintaining the pole in an upright position is of primary importance.

To the best of our knowledge, a fast TSMC has not been applied while utilizing TVSS for decoupled systems. Therefore, in this paper, we propose a type of fast, nonsingular, terminal, decoupled, SMC (FNTDSMC) that uses TVSS for the control of a class of fourth-order, nonlinear systems. The proposed sliding surfaces utilize time-varying coefficients, continuously computed via linear functions. The linear functions are derived from the input-output mapping of a 1-D fuzzy rule base, as in [24]. This enables fast convergence of the system states to the sliding surface. Decoupling of the subsystems is realized by embedding the target of the secondary subsystem into the primary subsystem via an intermediate signal in the manner of [25]. The proposed FNTDSMC system exhibits a considerable improvement in terms of faster transient response and lower error values as compared with the existing decoupled control methods.

2. Problem formulation

Many classical control algorithms are formulated as nonlinear, second-order systems, which can be expressed by [11, 12]:

$$\begin{aligned} \dot{x}_1 &= x_2, \\ \dot{x}_2 &= f(\mathbf{x}) + b(\mathbf{x})\, u + d(t), \\ y &= x_1 \quad , \end{aligned} \tag{1}$$

where $\mathbf{x} = [x_1, x_2]^{\mathrm{T}}$ is the state vector, $f(\mathbf{x})$ and $b(\mathbf{x})$ are nonlinear functions representing system dynamics, $d(t)$ is an external disturbance bounded as $|d(t)| \leq D$, u is the scalar control input, and y is the scalar output. Such systems are called single-input, single-output systems.

Special forms of Eq. (1) are commonly used to model and control more complex systems, such as those with multiple inputs and/or outputs. In this paper, we consider single-input, multioutput, underactuated, fourth-order systems that can be modeled as [25–28]:

$$\begin{aligned} \dot{x}_1 &= x_2, \\ \dot{x}_2 &= f_1(\mathbf{x}) + b_1(\mathbf{x})\, u + d_1(t), \\ \dot{x}_3 &= x_4, \\ \dot{x}_4 &= f_2(\mathbf{x}) + b_2(\mathbf{x})\, u + d_2(t), \\ y &= [x_1, x_3]^{\mathrm{T}} \quad , \end{aligned} \tag{2}$$

where x_1, x_3, and u denote the two outputs and a single input, respectively; $\mathbf{x} = [x_1, x_2, x_3, x_4]^{\mathrm{T}}$ is the state vector; and $d_1(t)$ and $d_2(t)$ represent external disturbances bounded as $|d_i(t)| \leq D$, $i = 1, 2$. Here, $f_i(\mathbf{x})$ and $b_i(\mathbf{x})$, $i = 1, 2$, represent the nonlinear dynamics of the system. The system described by Eq. (2) could represent, in particular, a cart-pole inverted pendulum system [25]. For a cart-pole system, for example, x_1, x_3, and u represent the pole angular position, cart position, and force exerted on the cart, respectively.

The aim here is to devise a control strategy that can control the type of system represented by Eq. (2) to improve on the convergence and robustness performances achieved by the prior cart. However, there are two inherent difficulties with this: (i) having fewer actuators than degrees of freedom increases the difficulty of the control algorithm; and (ii) the simultaneous control of each individual subsystem is difficult, so in the above cart-pole example, the controller will be designed to control either the cart or the pole. A well-known and effective approach to tackling this problem is to apply a two-level decoupling strategy (as in [25]) that would decouple the coupled system of Eq. (2) into Eq. (1); see Section 3.3.

3. Review of existing control methods

3.1. Terminal sliding-mode control

For second-order systems, as in Eq. (1), conventional TSMC uses nonlinear sliding surfaces [14, 15], e.g.,

$$s = \lambda\, {x_1}^{(p/q)} + x_2 \quad , \tag{3}$$

where $p, q \in \mathbb{Z}$ are positive and odd, satisfying $p < q$, and the sliding surface parameter $\lambda > 0$ becomes a parameter replacing the slope of the classical linear sliding-surface function [11]. For the TSMC sliding surface, it has been shown that the time to reach the equilibrium is [16]:

$$t_r = \frac{1}{\lambda\,(1 - p/q)}\, \left|x_1(0)\right|^{1-(p/q)} \quad . \tag{4}$$

It is evident from Eq. (4) that the system enters the terminal sliding mode in finite time. This is in contrast to SMC where finite-time convergence is not guaranteed. It is known that the classical TSMC suffers from the singularity problem, occurring for the case $x_1 = 0$ and $x_2 \neq 0$ [17, 20], which needs to be addressed.

3.2. Fast nonsingular terminal sliding-mode control

Although faster convergence is achieved when the system state is near equilibrium, TSMC may exhibit much slower convergence for the case where the state trajectory is far from equilibrium [19]. To address this issue fast nonsingular TSMC (FNTSMC) has been proposed, which also avoids the singularity problem. For second-order systems, the FNTSMC sliding-surface function is [6]:

$$s = \lambda \, |x_1|^{(p/q)} \, \mathrm{sgn}(x_1) + \alpha \, x_1 + x_2 \quad , \tag{5}$$

where the proportional term $\alpha > 0$ is used to achieve faster convergence when the state is away from the origin. It is well known that the convergence time for FNTSMC is [6]:

$$t_r = \frac{1}{\alpha \, (1 - p/q)} \, \ln \frac{\alpha \, \left|x_1(0)\right|^{1-(p/q)} + \lambda}{\lambda} \quad . \tag{6}$$

Motivated by the work in [28], the effect of the additional proportional term on the performance of the controller can be analyzed by simulating both Eqs. (4) and (6). To this end, a plot of λ versus convergence time t_r is shown in Figure 1 for $\alpha = 3$. We see that by increasing the value of the sliding-mode parameter λ, the convergence speed of both techniques improves. Moreover, it is clear that the fast term in FNTSMC unlocks performance regions, in terms of reduction in convergence time, that are unreachable to TSMC.

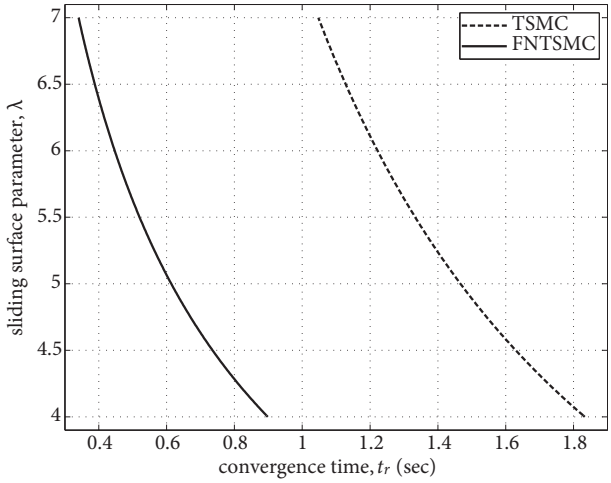

Figure 1. Convergence time t_r for different λ values.

3.3. Decoupled control

An effective way of controlling two subsystems, e.g., Eq. (2), simultaneously is through the use of a two-level decoupling strategy, or DSMC, [25]. This can be realized by first identifying the primary subsystem: the system for which the controller is designed with the main objective in mind. Then state information regarding the secondary subsystem is embedded into the primary subsystem via an intermediate signal, z. The sliding surface s_1 related to the primary subsystem is given by [25]:

$$s_1 = \lambda_1 \, (x_1 - z) + x_2 \quad , \tag{7}$$

and z is defined as

$$z = \text{sat}\left(\frac{s_2}{\phi_z}\right) z_u \ , \quad 0 < z_u < 1 \ , \tag{8}$$

where $\phi_z > 1$,

$$\text{sat}(\varphi) = \begin{cases} \text{sgn}(\varphi), & \text{if } |\varphi| \geq 1 \\ \varphi, & \text{if } |\varphi| < 1, \end{cases} \tag{9}$$

is the saturation function. Here, $\text{sgn}(\varphi)$ is the sign function [29] and s_2 is the sliding-surface function for the secondary subsystem, given by

$$s_2 = \lambda_2 \, x_3 + x_4 \quad , \tag{10}$$

where $\lambda_1, \lambda_2 > 0$. Intuitively, ϕ_z scales down s_2 into an appropriate range for s_1, and z_u imposes an upper bound on z, which makes for an effective way of transferring state information between the subsystems.

Note that since the sliding function s_1 in Eq. (7) is defined in terms of the intermediate signal, the objective of the controller is $x_1 = z$ and $x_2 = 0$, instead of $x_1 = 0$ and $x_2 = 0$.

3.4. Time-varying sliding surfaces

Previous works have focused on the adaptive selection of the sliding surface parameter λ for the purpose of shortening the reaching-mode duration and thus achieving faster convergence to the sliding mode [8, 21–24]. In particular, application of fuzzy-logic schemes have shown success in calculating the sliding-surface slope [23, 24]. An efficient 1-D fuzzy rule base was proposed that effectively adjusts the slope of the linear sliding surface of second- and fourth-order systems in [24, 27]. In [8], Komurcugil used the 1-D fuzzy rule base to reduce the reaching mode duration in the control of single-phase UPS inverters.

This rule base is reproduced in Table 1, and the linguistic fuzzy rule is:

Table 1. One-dimensional rule base used to adjust λ.

X_d	NB	NM	NS	ZR	PS	PM	PB
$\mathbf{\Lambda}$	VVB	VB	B	M	S	VS	VVS

$$\text{IF } x_d \text{ is } X_d \text{ THEN } \lambda \text{ is } \mathbf{\Lambda}, \tag{11}$$

where

$$X_d = |X_1| - |X_2| \quad , \tag{12}$$

where X_1, X_2, and $\mathbf{\Lambda}$ are "fuzzified" forms of the crisp variables x_1, x_2, and λ, respectively.

During the control process, the corresponding fuzzy values for x_1 and x_2 are used with the fuzzy inference system for successful operation. The output membership functions, $\mathbf{\Lambda}$, are confined to the set $\{\mathbf{\Lambda} \mid 0 \leq \mathbf{\Lambda} \leq 2\}$, which produces a positive sliding-surface slope and maintains system stability. By restricting the midpoint of output membership functions to unity we ensure that, after the transient period, the time-varying λ will be equal to the equivalent fixed parameter used by the traditional SMC/TSMC. The fuzzy input membership functions are labeled as negative-big (NB), negative-medium (NM), negative-small (NS), zero (ZR), positive-small (PS), positive-medium (PM), and positive-big (PB), whereas the fuzzy output membership functions are

denoted by very-very-small (VVS), very-small (VS), small (S), medium (M), big (B), very-big (VB), and very-very-big (VVB). Each membership function is an isosceles triangle. These membership functions are uniformly distributed with a 50% overlap. For more detail, the reader is referred to [24].

This set of fuzzy rules has been shown to provide a very efficient fuzzy inference system as compared to systems employing 2-D fuzzy rule bases [12, 23]. The control surface generated by this 1-D fuzzy system can be approximated by the following linear equation [24]:

$$\lambda_c = G_3\Big(-0.9\ \big(|G_1\ x_1| - |G_2\ x_2| \big) + 1 \Big) \quad , \tag{13}$$

where G_1, G_2, and G_3 are, respectively, the input and output scaling gains of the fuzzy system, and λ_c is referred to as the "crisp" lambda value. The implicit linearization eliminates the need for the fuzzy rules, significantly reducing the computational complexity and memory requirements.

4. Proposed control method

4.1. Fast nonsingular terminal decoupled SMC

In this subsection, a controller for the coupled, fourth-order, nonlinear system defined in Eq. (2) is described. Our control method is based on a synergistic combination of the following: (i) the decoupling method in [25]; (ii) the reaching law method in [30]; (iii) fast, nonsingular TSMC in [6]; and (iv) time-varying sliding surfaces in [24].

We now define a new decoupled TSMC law that incorporates a fast term for expediting state-trajectory movement to the equilibrium point, namely the fast, nonsingular, terminal, decoupled, sliding-mode controller (FNTDSMC). The corresponding nonlinear sliding surface functions are given by:

$$s_1 = \lambda_1\ |x_1 - z|^{(p_1/q_1)}\ \mathrm{sgn}(x_1 - z) + \alpha_1\ (x_1 - z) + x_2 \tag{14}$$

and

$$s_2 = \lambda_2\ |x_3|^{(p_2/q_2)}\ \mathrm{sgn}(x_3) + \alpha_2\ x_3 + x_4 \quad , \tag{15}$$

where λ_1 and λ_2 are the sliding-surface parameters and $\alpha_1, \alpha_2 > 0$ are the FNTSMC parameters, akin to that in Eq. (5). Here, the intermediate signal z is defined as in Eq. (8).

Upon reaching the terminal sliding mode, system dynamics are restricted to the sliding surface $s_1 = 0$ according to Eq. (14). Hence, we obtain the first-order nonlinear differential equation given by

$$\dot{x}_1 = -\lambda_1\ |x_1 - z|^{(p_1/q_1)}\ \mathrm{sgn}(x_1 - z) - \alpha_1\ (x_1 - z)\ . \tag{16}$$

Extending Eq. (6), the primary subsystem converges to the equilibrium point in the following time:

$$t_{s_1} = \frac{1}{\alpha_1\ (1 - p_1/q_1)}\ \ln \frac{\alpha_1\ \big|x_1(0) - z(0)\big|^{1-(p_1/q_1)} + \lambda_1}{\lambda_1}\ . \tag{17}$$

Note that the secondary subsystem also converges at the same due to the utilized decoupling method.

Hence, the proposed control law is given by

$$u = -b_1^{-1}(\mathbf{x})\Big(\lambda_1\ \frac{p_1}{q_1}\ |x_1 - z|^{(p_1/q_1)-1}\ (\dot{x}_1 - \dot{z}) + \alpha_1\ (\dot{x}_1 - \dot{z}) + f_1(\mathbf{x}) + k_1\ s_1 + k_2\ |s_1|^{\rho}\ \mathrm{sgn}(s_1) \Big)\ , \tag{18}$$

where $k_1, k_2 > 0$ and $0 < \rho < 1$ are the parameters of the switching function of the reaching-law method [30]. Moreover, parameters λ_1 and λ_2 are continually updated by utilizing the time-varying sliding-surface method described in Section 3.4. The essential control-flow of the proposed method can be gathered from the block diagram in Figure 2.

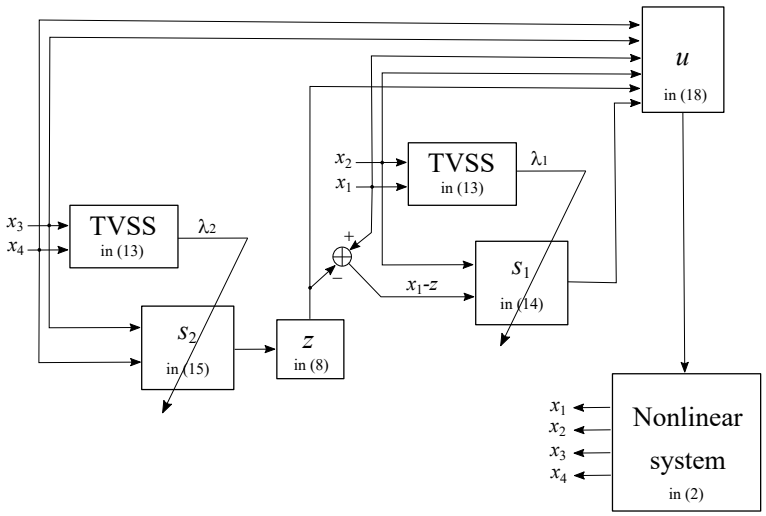

Figure 2. Block diagram of the proposed control method.

4.2. Stability analysis

A stability analysis of the proposed controller is provided in the following.

Theorem 1 *Consider the nonlinear fourth-order system in Eq. (2). If the control input is designed as in Eq. (18) and the sliding-surface functions in Eqs. (14) and (15) are used, then the state trajectory will converge to the equilibrium point in finite time.*

Proof Consider the following Lyapunov function [29]:

$$V = \frac{1}{2}\, {s_1}^2 \quad . \tag{19}$$

Using Eq. (18) in the time-derivative of Eq. (19), we get

$$\begin{aligned} \dot{V} &= s_1\, \dot{s}_1 \\ &= s_1 \left(-\, k_1\, s_1 - k_2\, |s_1|^{\rho}\, \mathrm{sgn}(s_1) + d_1(t) \right) <\ 0\ . \end{aligned} \tag{20}$$

Provided $k_1 > 0$, $k_2 > D$, Eq. (20) is a sufficient condition for the system state to reach the sliding surface, s_1, and converge to equilibrium in finite time according to the Lyapunov stability criterion [29].

Hence, we have $s_1 = 0$ and $\dot{s}_1 = 0$ during the terminal sliding mode. To get $s_1 \to 0$, we need $x_1 \to z$ and $x_2 \to 0$. Therefore, we require that z converges to zero in finite time so that both subsystems converge to the equilibrium point. To show $z \to 0$ we use Eq. (14) and the fact $\dot{s}_1 = 0$; that is,

$$0 = \lambda_1\, \frac{p_1}{q_1}\, |x_1 - z|^{(p_1/q_1)-1}\, (\dot{x}_1 - \dot{z}) + \alpha_1\, (\dot{x}_1 - \dot{z}) + \dot{x}_2, \tag{21}$$

which can be rewritten as

$$\dot{x}_2 = -\lambda_1 \frac{p_1}{q_1} |x_1 - z|^{(p_1/q_1)-1} x_2 - \alpha_1 x_2 + \lambda_1 \frac{p_1}{q_1} |x_1 - z|^{(p_1/q_1)-1} \dot{z} + \alpha_1 \dot{z} \quad . \tag{22}$$

The differential equation above can be solved for x_2 as

$$\begin{aligned} x_2(t) = x_2(0)\, e^{-\int \alpha_1 + \lambda_1 \gamma_1 |x_1 - z|^{\gamma_1 - 1} d\xi} + \alpha_1 \int_0^t e^{-\int \alpha_1 + \lambda_1 \gamma_1 |x_1 - z|^{\gamma_1 - 1} d\xi} \dot{z}\, d\tau \\ + \lambda_1 \gamma_1 \int_0^t e^{-\int \alpha_1 + \lambda_1 \gamma_1 |x_1 - z|^{\gamma_1 - 1} d\xi} \dot{z} |x_1 - z|^{\gamma_1 - 1} d\tau \quad , \end{aligned} \tag{23}$$

where $\gamma_1 = (p_1/q_1)$.

From Eq. (23), we see that $x_2 \to 0$ is guaranteed if and only if $x_1 \to z$ and $\dot{z} \to 0$. The two conditions are satisfied due to the following reasoning:

1. The sliding function s_1 is bound to go to zero since our control law is based on this function. This implies that $x_1 \to z$.
2. From Eq. (8), we see that z is a bounded oscillatory signal that decays to zero [25].

Furthermore, since $z \to 0$, $s_2 \to 0$; therefore, $x_3 \to 0$ and $x_4 \to 0$, as has been attested similarly in [25–28].

□

5. Numerical simulations

In this section, we verify the performance and effectiveness of the proposed fast terminal DSMC approach on two classic problems: a cart-pole system and ball-beam system [25]. For the cart-pole problem, we compare the performance of our system with that of nonsingular terminal DSMC (NTDSMC) in [28], TVSS in [27], and DSMC in [25], whereas in the case of the ball-beam problem the performance of the proposed method is compared to that of DSMC only, for the sake of brevity. Numerical simulations are carried out in the MATLAB-Simulink environment, with a fixed step size of 5 ms, which has been set up so as to facilitate a fair comparison with the results from simulations conducted in [25, 27, 28].

5.1. Measures

In this subsection, we define two metrics that are used to assess the error in the time evolution of our control system. These are the integral absolute error (IAE),

$$\text{IAE} = \int_0^\infty |e(t)|\, dt \,, \tag{24}$$

and the integral time-weighted absolute error (ITAE),

$$\text{ITAE} = \int_0^\infty t\, |e(t)|\, dt \,, \tag{25}$$

where

$$e_i(t) = r_i(t) - y_i(t) \,, \quad i = 1, 2 \,, \tag{26}$$

$r_i(t) = 0$, $y_1(t) = x_1$, and $y_2(t) = x_3$.

5.2. Results

5.2.1. Inverted pendulum

Consider the cart-pole inverted pendulum system, as illustrated in Figure 3. The equations of motion describing this system are [25]:

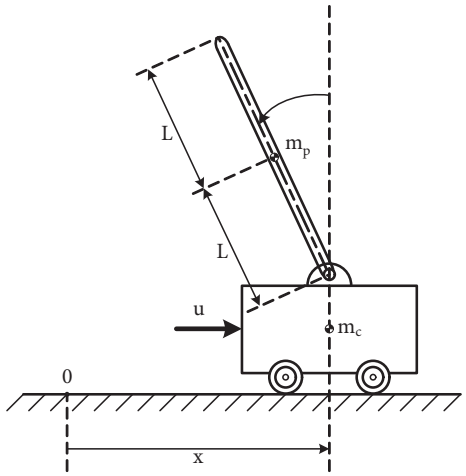

Figure 3. The cart-pole inverted pendulum system.

$$\begin{aligned}
\dot{x}_1 &= x_2, \\
\dot{x}_2 &= f_1(\mathbf{x}) + b_1(\mathbf{x})\, u + d_1(t), \\
\dot{x}_3 &= x_4, \\
\dot{x}_4 &= f_2(\mathbf{x}) + b_2(\mathbf{x})\, u + d_2(t) \quad ,
\end{aligned} \tag{27}$$

where

$$\begin{aligned}
f_1(\mathbf{x}) &= \frac{m_t\, g \sin(x_1) - m_p\, L \sin(x_1) \cos(x_1)\, {x_2}^2}{L\big(\frac{4}{3}\, m_t - m_p \cos^2(x_1)\big)}, \\
b_1(\mathbf{x}) &= \frac{\cos(x_1)}{L\big(\frac{4}{3}\, m_t - m_p \cos^2(x_1)\big)}, \\
f_2(\mathbf{x}) &= \frac{-\frac{4}{3}\, m_p\, L\, {x_2}^2 \sin(x_1) \; + m_p\, g \sin(x_1) \cos(x_1)}{\frac{4}{3}\, m_t - m_p \cos^2(x_1)}, \\
b_2(\mathbf{x}) &= \frac{4}{3\big(\frac{4}{3}\, m_t - m_p \cos^2(x_1)\big)} \quad .
\end{aligned} \tag{28}$$

Here, x_1 is the pole angular position from the vertical axis, x_2 is the pole angular velocity with respect to the vertical axis, x_3 is the cart position from the reference point, x_4 is the cart velocity, L is the pole half-length, and m_t is the total mass of the system, which comprises the pole mass m_p and the cart mass m_c. The primary subsystem is formed by the state variables x_1 and x_2, whereas the secondary subsystem is formed by the state variables x_3 and x_4, thus enabling the applicability of the proposed control method. The aim is to maintain the pole in an upright position.

Parameters related to the system under study are presented in Table 2. The parameters used for the control methods assessed in this paper are given in Table 3. Note that parameters used here were chosen in order to conduct a fair comparison with previous works, particularly [25, 27, 28].

Table 2. Parameters of the cart-pole system.

m_p	m_c	L	g	d_1 & d_2
0.05 kg	1 kg	0.5 m	9.8 m/s^2	≤ 0.0873

Table 3. Controller specifications used in the cart-pole simulations.

	DSMC	TVSS	NTDSMC	Proposed method
λ_1/λ_2	5/0.5	-	-	-
K	10	-	-	-
Φ_1/Φ_z	5/15	-/15	-/15	-/15
z_U	0.9425	0.9425	0.9425	0.9425
G_1/G_2	-	1/40	-	-
$G_3/G_4/G_5$	-	0.05/0.05/5	0.05/0.05/5	0.05/0.05/5
$G_6/G_7/G_8$	-	0.05/0.05/0.5	0.05/0.05/0.5	0.05/0.05/0.5
p_1/q_1	-	-	19/21	19/21
p_2/q_2	-	-	17/21	17/21
ρ	-	-	0.8	0.8
k_1/k_2	-	-	10/10	10/10
α_1/α_2	-	-	-	2.9/0.1

Figures 4 and 5 depict system transient performances in terms of the pole angle and cart position, respectively. This is for an initial pole angle of $x_1(0) = -60^{\circ}$. Also included are the transient behaviors of the aforementioned prior cart. It can be seen that the proposed controller compares favorably to the other methods since it converges to the desired (steady-state) angular/cart position faster. Lower steady-state errors are also achieved by our method. For the angular position, accuracy was determined by considering the point at which angular positions fall and remain within 1° from the upright position; specifically, the proposed system achieves this 24% sooner compared to NTDSMC.

Notice also the marked improvement over the DSMC method. The fast response can be attributed to the fast terms in Eqs. (14) and (15), which are applied to the system during the controller's reaction to the displaced pole. Another striking result is that, despite this extremely short rise time, maximum overshoots exhibited by our method are similar to those of the state-of-the-art.

In Figure 6, we show the control input to the different control systems. It can be seen that our fast NTDSMC generates control inputs in a shorter period of time compared to the state-of-the-art. However, it is clear that a larger force is generated by our method; this is required in order to stabilize the pole in an upright position, meanwhile keeping the cart at the origin. There is a clear trade-off between the required control action and speed of convergence.

The evolution of coefficients λ_1 and λ_2 is shown in Figure 7, from which we see the time-varying

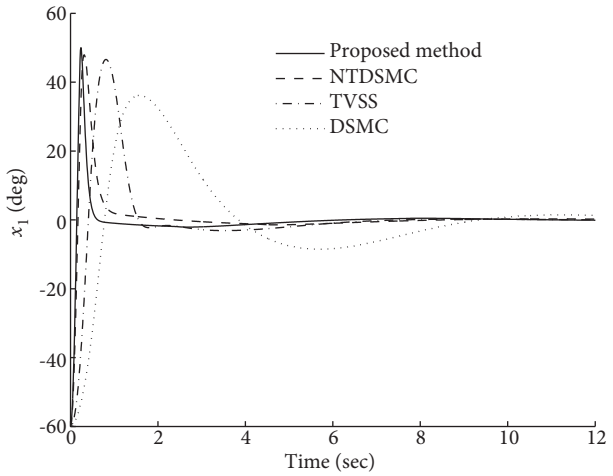

Figure 4. System-response comparison in terms of the angular position of the pole.

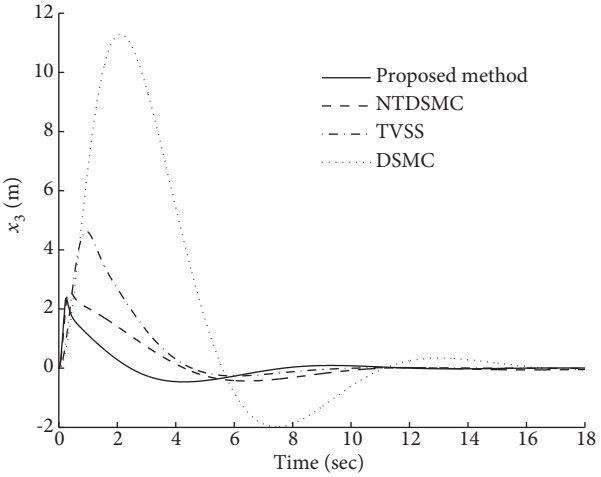

Figure 5. System-response comparison in terms of the position of the cart.

behavior of these parameters associated with our method, TVSS, and NTDSMC. Notice also that, in contrast, the coefficients of the DSMC method are constant. On further inspection, it is clear that λ_1 and λ_2, for the proposed method, settle to steady-state values of 5 and 0.5, respectively, slightly faster than the coefficients related to NTDSMC and TVSS; this is again a testament to the effectiveness of the new fast term of our controller. Interestingly, the slopes for λ_1 and λ_2 seem to change in accordance with the forces required in stabilizing the pole and cart.

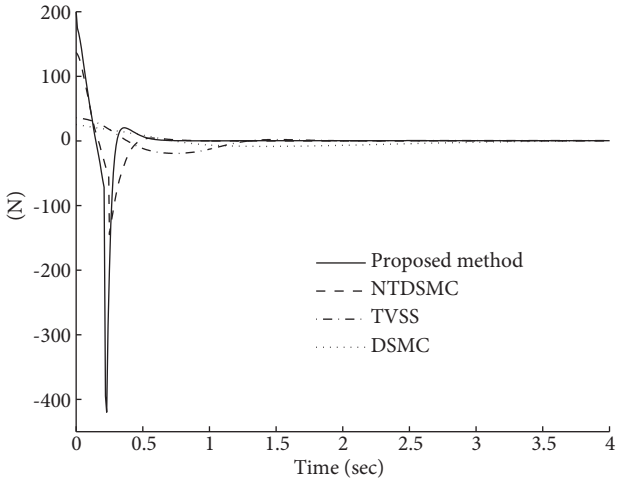

Figure 6. System-response comparison in terms of the required control input, as defined in Eq. (18), for the cart-pole system.

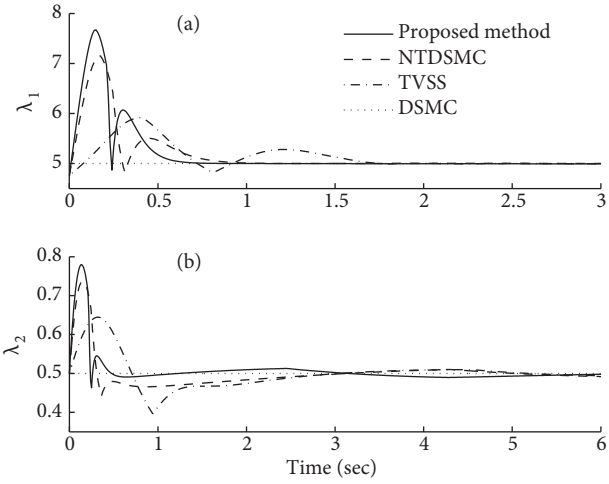

Figure 7. Time evolution of the sliding surface coefficients, (a) λ_1 and (b) λ_2, for the various controllers related to the cart-pole system.

In order to back up the qualitative results presented thus far, we provide quantitative analysis utilizing the metrics defined in Eqs. (24) and (25). The IAE and ITAE performances of the different methods are tabulated in Table 4. It is evident that the proposed method compares favorably with the state-of-the-art methods.

Finally, pole angular position and cart position are shown in Figure 8a and Figure 8b, respectively, for the abrupt disturbances in Figure 9. The amplitudes of d_1 and d_2 are 0.15 and 0.3 with 1% and 2% duty-cycles

Table 4. IAE and ITAE values obtained in the cart-pole simulations.

		DSMC	TVSS	NTDSMC	Proposed method
Angle	IAE	125.69	57.48	28.90	22.62
	$ITAE$	370.46	75.79	46.06	39.12
Position	IAE	42.29	9.84	7.16	3.98
	$ITAE$	156.24	20.41	24.41	12.06

applied at 20, 30, and 40 s, respectively. As can be seen, the proposed control method manages to successfully recover to a low-error steady-state condition after the occurrence of abrupt disturbances. The zoomed inset plots in these figures reveal the small-amplitude ripples present in the responses immediately after a step change in disturbance. Although not a demonstration of disturbance rejection, these results indicate that our method has the ability to suppress the effects of external disturbances to a good degree.

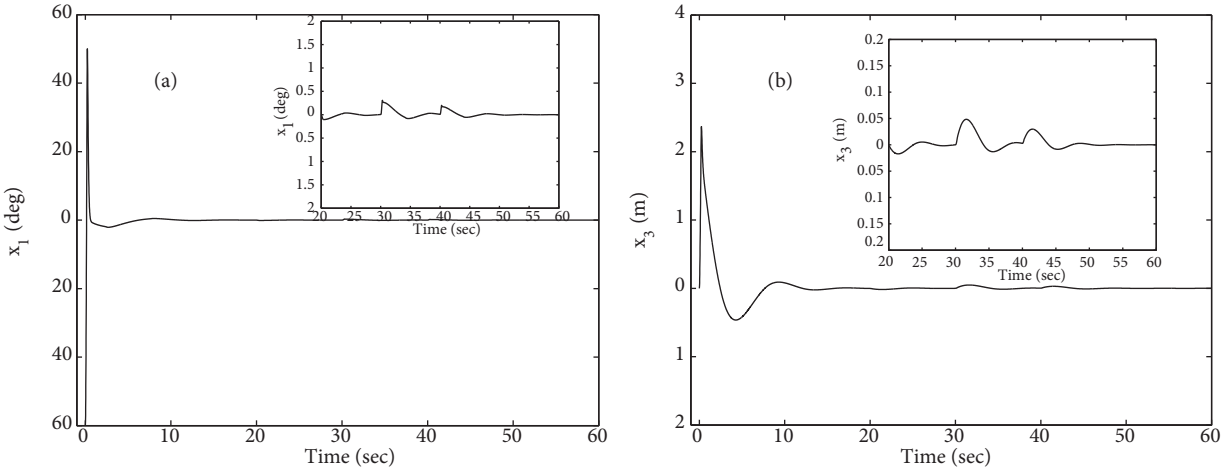

Figure 8. Position response for the (a) pole angle and (b) cart when disturbances are applied to the proposed controller.

5.2.2. Ball-beam system

The structure of the ball-beam system is shown in Figure 10. The systems dynamics are expressed by [25]:

$$\begin{aligned} \dot{x}_1 &= x_2, \\ \dot{x}_2 &= u, \\ \dot{x}_3 &= x_4, \\ \dot{x}_4 &= B\left(x_3\, {x_2}^2 - g\sin(x_1)\right) \quad , \end{aligned} \tag{29}$$

where x_1 is the angular position of the beam with respect to the horizontal axis, x_2 is the angular velocity of the beam, x_3 is the position of the ball, and x_4 is the velocity of the ball. B is defined as $B = \frac{M\ R^2}{J_b\ M\ R^2}$, where J_b is the moment of inertia of the ball.

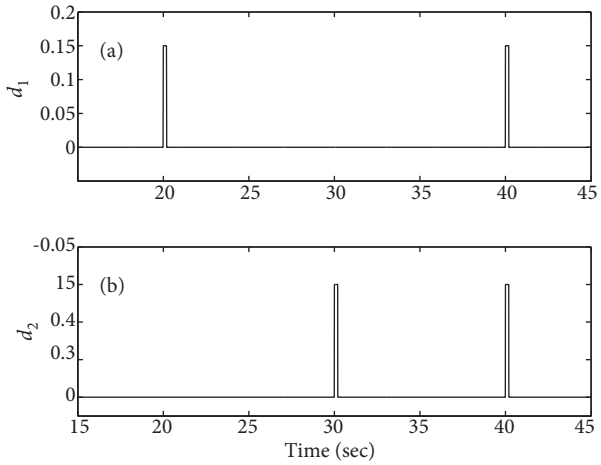

Figure 9. External disturbances (a) d_1 and (b) d_2 used in our studies of the cart-pole system.

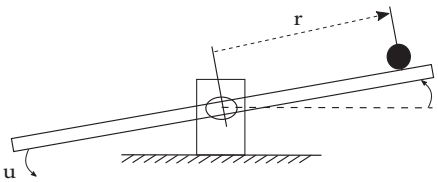

Figure 10. The ball-beam system.

The aim is twofold: to maintain (i) a horizontal beam position and (ii) a centered ball. This is sought after with the following assumptions: (i) the beam and ball are continually in contact; (ii) rolling occurs without slipping; (iii) there are no obstructions in the ball path; and (iv) the center of rotation is frictionless.

Parameters related to the ball-beam system are given in Table 5. The parameters used for the control methods assessed in this paper are given in Table 6. Again, parameters were chosen with a view to conducting a fair comparison with previous works, particularly [25].

Table 5. Parameters of the ball-beam system.

M	R	J_b	g
0.05 kg	0.01 m	2×10^{-6}	9.8 m/s^2

With an initial beam-angle of $x_1(0) = 60^o$ and ball position of $x_3(0) = 10$ m, the evolution of the beam angular position is shown for both the proposed and DSMC methods in Figure 11. The error metrics for the two methods are provided in Table 7. A striking result is that the significant performance gains obtained by the proposed method for the cart-pole problem cannot be observed in the case of the ball-beam system. The lackluster performance is essentially due to the fact that the input features in only one of the states of the ball-beam system dynamics. Therefore, the input feeds through to only one of the decoupled subsystems. On the other hand, the input to the cart-pole is able to influence both the decoupled subsystems, which is exploited by our method, and in fact all DSMC-type approaches in general. This analysis has revealed that control methods based on the decoupled SMC approach can be sensitive to the dynamics of the problem, and in particular the availability of input-related information in both subsystems.

6. Conclusions

In this paper, a novel form of fast SMC is proposed for application to a class of fourth-order, nonlinear systems. Our controller combines the benefits of decoupled control and terminal SMC, together with efficient fuzzy-based, time-varying sliding surfaces, while avoiding the problem of singularity. Compared to the state-of-the-art, the proposed method establishes faster convergence of state trajectories to the equilibrium point.

Table 6. Controller specifications used in the ball-beam simulations.

	DSMC	Proposed method
λ_1/λ_2	10/0.5	-
K	10	-
Φ_1/Φ_z	5/5	-/5
z_U	0.9425	0.9425
G_1/G_2	-	-
$G_3/G_4/G_5$	-	0.01/0.01/10
$G_6/G_7/G_8$	-	0.01/0.01/0.5
p_1/q_1	-	19/21
p_2/q_2	-	19/21
ρ	-	0.8
k_1/k_2	-	10/10
α_1/α_2	-	0.2/0.2

Table 7. IAE and ITAE values obtained in the ball-beam simulations.

		DSMC	Proposed method
Angle	IAE	95.84	86.64
	$ITAE$	178.25	156.84
Position	IAE	19.77	22.52
	$ITAE$	27.44	33.96

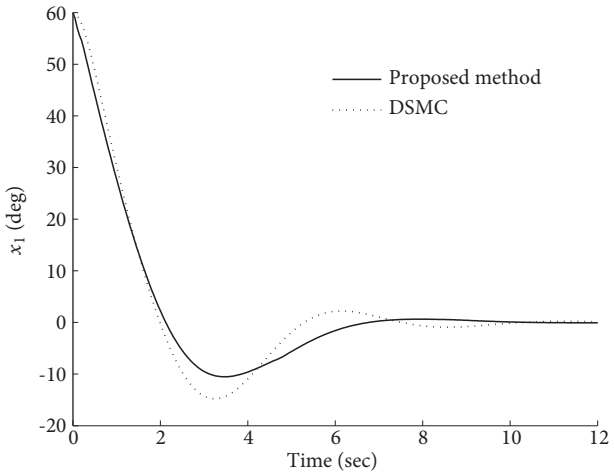

Figure 11. System-response comparison in terms of the angular position of the beam.

Using the Lyapunov stability theorem, we have derived sufficient conditions that guarantee the asymptotic boundedness of system states while taking into account external disturbances. In the case of the cart-pole system, superior convergence performance has been demonstrated through computer simulations, whereas comparable

performances were observed for the ball-beam system. Future work will consist of adapting and applying our controller to more general problems in control and optimization.

References

[1] Zuo Z. Non-singular fixed-time terminal sliding mode control of non-linear systems. Automatica 2015; 9: 545-552.

[2] Mobayen S. Fast terminal sliding mode tracking of non-holonomic systems with exponential decay rate. IET Control Theory Appl 2015; 9: 1294-1301.

[3] Kizir S, Bingul Z, Oysu C. Fuzzy control of a real time inverted pendulum system. J Intell Fuzzy Syst 2010; 21: 121-133.

[4] Roose AI, Yahya S, Al-Rizzo H. Fuzzy-logic control of an inverted pendulum on a cart. Comput Electr Eng 2017; 61: 31-47.

[5] Yang L, Yang J. Nonsingular fast terminal sliding-mode control for nonlinear dynamical systems. Int J Robust Nonlinear Control 2011; 21: 1865-1879.

[6] Yu S, Yu X, Shirinzadeh B, Man Z. Continuous finite-time control for robotic manipulators with terminal sliding mode. Automatica 2005; 41: 1957-1964.

[7] Xu SSD, Chen CC, Wu ZL. Study of nonsingular fast terminal sliding-mode fault-tolerant control. IEEE T Ind Electron 2015; 62: 3906-3913.

[8] Komurcugil H. Rotating-sliding-line based sliding-mode control for single-phase UPS inverters. IEEE T Ind Electron 2012; 59: 3719-3726.

[9] Yazici I, Yaylaci EK. Fast and robust voltage control of DC-DC boost converter by using fast terminal sliding mode controller. IET Power Electron 2015; 9: 120-125.

[10] Al-Ghanimi A, Zheng J, Man Z. Robust and fast non-singular terminal sliding mode control for piezoelectric actuators. IET Control Theory Appl 2015; 9: 2678-2687.

[11] Hung JY, Gao W, Hung JC. Variable structure control: a survey. IEEE T Ind Electron 1993; 40: 2-22.

[12] Yu X, Kaynak O. Sliding-mode control with soft computing: a survey. IEEE T Ind Electron 2009; 56: 3275-3285.

[13] Slotine JJ, Sastry SS. Tracking control of non-linear systems using sliding surfaces, with application to robot manipulators. Int J Control 1983; 38: 465-492.

[14] Venkataraman ST, Gulati S. Control of nonlinear systems using terminal sliding modes. J Dyn Syst Meas Control 1993; 115: 554-560.

[15] Zhihong M, Paplinski AP, Wu HR. A robust MIMO terminal sliding mode control scheme for rigid robotic manipulators. IEEE T Autom Control 1994; 39: 2464-2469.

[16] Zak M. Terminal attractors for addressable memory in neural networks. Phys Lett A 1988; 133: 18-22.

[17] Park KG, Tsuji T. Terminal sliding mode control of second-order nonlinear uncertain systems. Int J Robust Nonlinear Control 1999; 9: 769-780.

[18] Feng Y, Yu X, Man Z. Non-singular terminal sliding mode control of rigid manipulators. Automatica 2002; 38: 2159-2167.

[19] Yu X, Zhihong M. Fast terminal sliding-mode control design for nonlinear dynamical systems. IEEE T Circuits-I 2002; 49: 261-264.

[20] Feng Y, Yu X, Han F. On nonsingular terminal sliding-mode control of nonlinear systems. Automatica 2013; 49: 1715-1722.

[21] Choi SB, Cheong CC, Park DW. Moving switching surfaces for robust control of second-order variable structure systems. Int J Control 1993; 58: 229-245.

[22] Bartoszewicz A. Time-varying sliding modes for second-order systems. IEE Proc-Control Theory Appl 1996; 143: 455-462.

[23] Yagiz N, Hacioglu Y. Fuzzy sliding modes with moving surface for the robust control of a planar robot. J Vib Control 2005; 11: 903-922.

[24] Yorgancioglu F, Komurcugil H. Single-input fuzzy-like moving sliding surface approach to the sliding mode control. Electr Eng 2008; 90: 199-207.

[25] Lo JC, Kuo YH. Decoupled fuzzy sliding-mode control. IEEE T Fuzzy Syst 1998; 6: 426-435.

[26] Hung LC, Chung HY. Decoupled control using neural network-based sliding-mode controller for nonlinear systems. Expert Syst Appl 2007; 32: 1168-1182.

[27] Yorgancioglu F, Komurcugil H. Decoupled sliding-mode controller based on time-varying sliding surfaces for fourth-order systems. Expert Syst Appl 2010; 37: 6764-6774.

[28] Bayramoglu H, Komurcugil H. Nonsingular decoupled terminal sliding-mode control for a class of fourth-order nonlinear systems. Commun Nonlinear Sci Numer Simul 2013; 18: 2527-2539.

[29] Slotine JJE, Li W. Applied Nonlinear Control. Englewood Cliffs, NJ, USA: Prentice Hall, 1991.

[30] Gao W, Hung JC. Variable structure control of nonlinear systems: a new approach. IEEE T Ind Electron 1993; 40: 45-55.